The Astrophysical Journal, 740:49 (6pp), 2011 October 10 doi:10.1088/0004-637X/740/1/49

55 CANCRI: STELLAR ASTROPHYSICAL PARAMETERS, A PLANET IN THE HABITABLE ZONE, AND IMPLICATIONS FOR THE RADIUS OF A TRANSITING SUPER-EARTH

Kaspar von Braun[1], Tabetha S. Boyajian[2,10], Theo A. ten Brummelaar[3], Stephen R. Kane[1], Gerard T. van Belle[4], David R. Ciardi[1], Sean N. Raymond[5,6], Mercedes López-Morales[7,8], Harold A. McAlister[2], Gail Schaefer[3], Stephen T. Ridgway[9], Laszlo Sturmann[3], Judit Sturmann[3], Russel White[2], Nils H. Turner[3], Chris Farrington[3], and P. J. Goldfinger[3]

[1] NASA Exoplanet Science Institute, California Institute of Technology, MC 100-22, Pasadena, CA 91125, USA; kaspar@caltech.edu
[2] Center for High Angular Resolution Astronomy and Department of Physics and Astronomy, Georgia State University, P. O. Box 4106, Atlanta, GA 30302-4106, USA
[3] The CHARA Array, Mount Wilson Observatory, Mount Wilson, CA 91023, USA
[4] European Southern Observatory, Karl-Schwarzschild-Str. 2, 85748 Garching, Germany
[5] Université de Bordeaux, Observatoire Aquitain des Sciences de l'Univers, 2 rue de l'Observatoire, BP 89, F-33271 Floirac Cedex, France
[6] CNRS, UMR 5804, Laboratoire d'Astrophysique de Bordeaux, 2 rue de l'Observatoire, BP 89, F-33271 Floirac Cedex, France
[7] Institut de Ciències de L'Espai (CSIC-IEEC), Campus UAB, Facultat Ciències, Torre C5 parell 2, 08193 Bellaterra, Barcelona, Spain
[8] Department of Terrestrial Magnetism, Carnegie Institution of Washington, 5241 Broad Branch Road, NW, Washington, DC 20015, USA
[9] National Optical Astronomy Observatory, P. O. Box 26732, Tucson, AZ 85726-6732, USA
Received 2011 June 1; accepted 2011 July 22; published 2011 September 26

ABSTRACT

The bright star 55 Cancri is known to host five planets, including a transiting super-Earth. The study presented here yields directly determined values for 55 Cnc's stellar astrophysical parameters based on improved interferometry: $R = 0.943 \pm 0.010\,R_{\odot}$, $T_{\rm EFF} = 5196 \pm 24$ K. We use isochrone fitting to determine 55 Cnc's age to be 10.2 ± 2.5 Gyr, implying a stellar mass of $0.905 \pm 0.015\,M_{\odot}$. Our analysis of the location and extent of the system's habitable zone (HZ; 0.67–1.32 AU) shows that planet f, with period ∼260 days and $M \sin i = 0.155\,M_{\rm Jupiter}$, spends the majority of the duration of its elliptical orbit in the circumstellar HZ. Though planet f is too massive to harbor liquid water on any planetary surface, we elaborate on the potential of alternative low-mass objects in planet f's vicinity: a large moon and a low-mass planet on a dynamically stable orbit within the HZ. Finally, our direct value for 55 Cancri's stellar radius allows for a model-independent calculation of the physical diameter of the transiting super-Earth 55 Cnc e ($\sim 2.05 \pm 0.15\,R_{\oplus}$), which, depending on the planetary mass assumed, implies a bulk density of $0.76\,\rho_{\oplus}$ or $1.07\,\rho_{\oplus}$.

Key words: infrared: stars – planetary systems – stars: fundamental parameters – stars: individual (55 Cnc) – stars: late-type – techniques: interferometric

Online-only material: color figure

1. INTRODUCTION

55 Cancri (= HD 75732 = ρ Cancri; 55 Cnc hereafter) is a late G/early K dwarf/subgiant (Gray et al. 2003) currently known to host five extrasolar planets with periods between around 0.7 days and 14 years and minimum masses between 0.026 and 3.84 $M_{\rm Jupiter}$ (Dawson & Fabrycky 2010). These planets were all discovered via the radial velocity method and successively announced in Butler et al. (1997), Marcy et al. (2002), McArthur et al. (2004), and Fischer et al. (2008).

Astrophysical insights on two of the currently known planets in the 55 Cnc system are direct consequences of the determination of the stellar radius and surface temperature.

1. Elimination of period aliasing and the consequently updated orbital scenario presented in Dawson & Fabrycky (2010) motivated the recent, successful photometric transit detections of the super-Earth 55 Cnc e with a period of 0.7 days by Winn et al. (2011) using Canadian Space Mission *Microvariability and Oscillations of Stars* (*MOST*) and, independently, by Demory et al. (2011) using Warm *Spitzer*. The calculation of planetary radii based on transit photometry relies, of course, on a measured or assumed stellar radius.
2. Based on the equations relating stellar luminosity to the location and extent of a stellar system's habitable zone (HZ; Jones & Sleep 2010), planet 55 Cnc f falls within 55 Cnc's traditional circumstellar HZ.

Apart from values derived from stellar modeling (Fischer et al. 2008), there are two direct (interferometric) stellar diameter determinations of 55 Cnc: $R = 1.15 \pm 0.035\,R_{\odot}$ in Baines et al. (2008) and $R = 1.1 \pm 0.096\,R_{\odot}$ in van Belle & von Braun (2009). Note, however, that van Belle & von Braun (2009) report, in their Sections 5.1 and 5.4.1, the fact that $R \sim 1.1\,R_{\odot}$ makes 55 Cnc a statistical outlier in their fitted $T_{\rm EFF} = f((V-K)_0)$ relation (see their Section 5.1). In order not to be an outlier, 55 Cnc's angular diameter would have to be 0.7 milliarcseconds (mas), corresponding to $0.94\,R_{\odot}$.

In this paper, we present new, high-precision interferometric observations of 55 Cnc with the aim of providing a timely, directly determined value of the stellar diameter, which, when combined with the flux decrement measured during planetary transit, yields a direct value for the exoplanetary diameter. Furthermore, the combination of angular stellar diameter and bolometric stellar flux provides directly determined stellar surface temperature. The resultant stellar luminosity determines the location and extent of the circumstellar HZ, and we can ascertain which, if any, of the planets orbiting 55 Cnc spend any, all, or part of their orbits inside the HZ.

[10] Hubble Fellow.

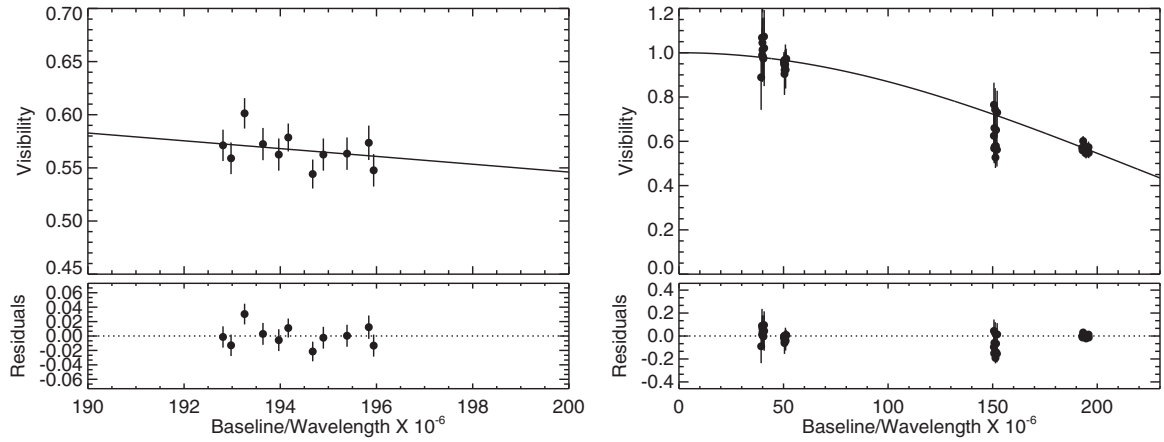

Figure 1. Calibrated visibility observations along with the limb-darkened angular diameter fit for 55 Cnc. The left panel shows the fit only based on the CHARA data presented in this work. For comparison with literature data sets, the right panel includes PTI data (shortest baseline) from van Belle & von Braun (2009), CHARA data from Baines et al. (2008; longer baseline), and data presented in this work (longest baseline), along with the same fit as in the left panel. The bottom panels show the residuals around the respective fit. Note the different scales for both *x*- and *y*-axes between the panels. For details, see Sections 2 and 3.1. The fit results are given in Table 1.

Table 1
Stellar Properties of 55 Cnc

Parameter	Value	Reference
Spectral type	K0 IV-V	Gray et al. (2003)
Parallax (mas)	81.03 ± 0.75	van Leeuwen (2007)
[Fe/H]	0.31 ± 0.04	Valenti & Fischer (2005)
$\theta_{\rm UD}$ (mas)	0.685 ± 0.004	This work (Section 2)
$\theta_{\rm LD}$ (mas)	0.711 ± 0.004	This work (Section 2)
Radius ($R_\odot$)	0.943 ± 0.010	This work (Section 3.1)
Luminosity ($L_\odot$)	0.582 ± 0.014	This work (Section 3.2)
$T_{\rm EFF}$ (K)	5196 ± 24	This work (Section 3.2)
Mass ($M_\odot$)	0.905 ± 0.015	This work (Section 3.3)
Age (Gyr)	10.2 ± 2.5	This work (Section 3.3)
log *g*	4.45 ± 0.01	This work (Section 3.3)
HZ boundaries (AU)	0.67–1.32	This work (Section 4)

Note. Directly determined and derived stellar parameters for the 55 Cnc system.

We describe our observations in Section 2. The determination of stellar astrophysical parameters is shown in Section 3. We discuss 55 Cnc's circumstellar HZ and the locations of the orbiting planets with respect to it in Section 4. Section 5 contains the calculation of the radius of the transiting super-Earth 55 Cnc e, and we conclude in Section 6.

2. INTERFEROMETRIC OBSERVATIONS

Our observational strategy is described in detail in von Braun et al. (2011a). We briefly repeat the general approach here.

55 Cnc was observed on the nights of 2011 May 11 and 12, using the Georgia State University Center for High Angular Resolution Astronomy (CHARA) Array (ten Brummelaar et al. 2005), a long baseline interferometer located at Mount Wilson Observatory in Southern California. We used the CHARA Classic beam combiner with CHARA's longest baseline, S1E1 ($\sim$ 330 m) to collect the observations in *H* band ($\lambda_{\rm central} = 1.67\,\mu$m).

The interferometric observations included the common technique of taking bracketed sequences of the object with calibrator stars, designed to characterize and subsequently eliminate the temporally variable effects of the atmosphere and telescope/instrument upon our calculation of interferometric visibilities.[11] During the observing period, we alternated between two point-source-like calibrators, both of which lie within 5 deg on the sky from the target, to minimize the systematic effects. These calibrator stars were HD 74811 (G2 IV; $\theta_{\rm EST} = 0.407 \pm 0.015$ mas) and HD 75332 (F8 V; $\theta_{\rm EST} = 0.401 \pm 0.014$ mas). $\theta_{\rm EST}$ corresponds the estimated angular diameter of the calibrator stars based on spectral energy distribution (SED) fitting.

The uniform disk and limb-darkened angular diameters $\theta_{\rm UD}$ and $\theta_{\rm LD}$[12], respectively, are found by fitting our calibrated visibility measurements to the respective functions for each relation (Hanbury Brown et al. 1974). Limb-darkening coefficients were taken from Claret (2000). The data and fit for $\theta_{\rm LD}$ are shown in the left panel of Figure 1.

3. FUNDAMENTAL ASTROPHYSICAL PARAMETERS OF THE STAR 55 CANCRI

In this section, we discuss 55 Cnc's stellar astrophysical properties. The results are summarized in Table 1.

3.1. Stellar Diameter

We examined the following two sets of literature interferometric data in order to decide whether to include them in our analysis: CHARA data presented in Baines et al. (2008) and data published in van Belle & von Braun (2009) taken with the Palomar Testbed Interferometer (PTI), which features a 110 m baseline compared to CHARA's 330 m.[13] In the left panel of Figure 1, we show our data and corresponding fit for $\theta_{\rm LD}$. The right panel of Figure 1 contains all three data sets along with the

[11] Visibility is the normalized amplitude of the correlation of the light from two telescopes. It is a unitless number ranging from 0 to 1, where 0 implies no correlation and 1 implies perfect correlation. An unresolved source would have perfect correlation of 1.0 independent of the distance between the telescopes (baseline). A resolved object will show a decrease in visibility with increasing baseline length. The shape of the visibility versus baseline is a function of the topology of the observed object (the Fourier transform of the object's shape). For a uniform disk this function is a Bessel function, and for this paper, we use a simple model of a limb-darkened variation of a uniform disk.

[12] The limb-darkening-corrected $\theta_{\rm LD}$ corresponds to the angular diameter of the Rosseland, or mean, radiating surface of the star.

[13] Canonically, CHARA's spatial resolution is therefore superior with respect to PTI data by a factor of three, but PTI data pipeline and its products are well characterized (Boden et al. 1998).

fit based on our new data. The superiority of our new CHARA data due to the longer baselines is readily apparent. We therefore chose to assign zero weight to the two literature data sets in our analysis, particularly due to the fact that fits inclusive of all data weighted equally do not influence the fit and corresponding results.

Our interferometric measurements (Figure 1) yield a limb-darkening-corrected angular diameter $\theta_{\rm LD} = 0.711 \pm 0.004$ mas. Combined with 55 Cnc's trigonometric parallax value from van Leeuwen (2007), we calculate its linear radius to be $R = 0.943 \pm 0.010\,R_{\odot}$ (Table 1).

Our result of $\theta_{\rm LD} \simeq 0.7$ mas is consistent with the PTI-derived value (∼1.1 mas) published in van Belle & von Braun (2009) at the 1.5σ level. Furthermore, $\theta_{\rm LD} \simeq 0.7$ mas exactly corresponds to the angular diameter required for 55 Cnc to fall onto the $T_{\rm EFF}$ versus $(V - K)_0$ relation in van Belle & von Braun (2009); see their Equation (2) and Section 5.4.1. Finally, our directly determined value for 55 Cnc's stellar radius ($R = 0.943\,R_{\odot}$) is consistent with the calculated value in Fischer et al. (2008) based on stellar parameters cataloged in Valenti & Fischer (2005).

3.2. Stellar Effective Temperature

Following the procedure outlined in Section 3.1 of van Belle et al. (2007), we produce a fit of the stellar SED based on the spectral templates of Pickles (1998) to literature photometry published in Niconov et al. (1957), Argue (1963, 1966), Marlborough (1964), Cowley et al. (1967), Rufener (1976), Persson et al. (1977), Eggen (1978), Olsen (1983, 1993), Mermilliod (1986), Arribas & Martinez Roger (1989), Gonzalez & Piche (1992), Hauck & Mermilliod (1998), Cutri et al. (2003), and Kazlauskas et al. (2005); see also the catalog of Gezari et al. (1999). Typical uncertainties per datum for these photometry data are in the range of 5%–8%.

We obtain fits with reduced $\chi^2 \sim 3$ when using K0 IV and G8 IV spectral templates. The creation of a G9 IV template by linearly interpolating the specific flux values of the K0 IV and G8 IV spectral templates for each value of λ, however, improves the quality of this fit to a reduced $\chi^2 = 0.72$. Interstellar extinction is a free parameter in the fitting process and produces a value of $A_V = 0.000 \pm 0.014$ mag, consistent with expectations for this nearby star. The value for the distance to 55 Cnc is adopted from van Leeuwen (2007). The SED fit for 55 Cnc, along with its residuals, is shown in Figure 2.

The principal result from the SED fit is the value of 55 Cnc's stellar bolometric flux of $F_{\rm BOL} = (1.227 \pm 0.0177) \times 10^{-7}$ erg cm^{-2} s^{-1}, and consequently, its luminosity of $L = 0.582 \pm 0.014\,L_{\odot}$. Using the rewritten version of the Stefan–Boltzmann law,

$$T_{\rm EFF}({\rm K}) = 2341 (F_{\rm BOL}/\theta_{\rm LD}^2)^{\frac{1}{4}}, \quad (1)$$

where $F_{\rm BOL}$ is in units of 10^{-8} erg cm^{-2} s^{-1} and $\theta_{\rm LD}$ is in units of mas, we calculate 55 Cnc's effective temperature to be $T_{\rm EFF} = 5196 \pm 24$ K.

3.3. Stellar Mass and Age

Our values for 55 Cnc's stellar luminosity and effective temperature are compared to Yonsei–Yale stellar isochrones (Demarque et al. 2004; Kim et al. 2002; Yi et al. 2001) with [Fe/H] = 0.31 (Valenti & Fischer 2005; Fischer et al. 2008) to estimate its mass and age. As illustrated in Figure 3, interpolating between isochrones and mass tracks yields a best-fit age of 55 Cnc of 10.2 ± 2.5 Gyr and stellar mass of $0.905 \pm 0.015\,M_{\odot}$. Note that the above uncertainties are based on only the 1σ measurement errors in our calculations of L (∼2.4%) and $T_{\rm EFF}$ (∼0.5%), shown as error bars in Figure 3, and do not take into account systematic offsets due to, e.g., metallicity.

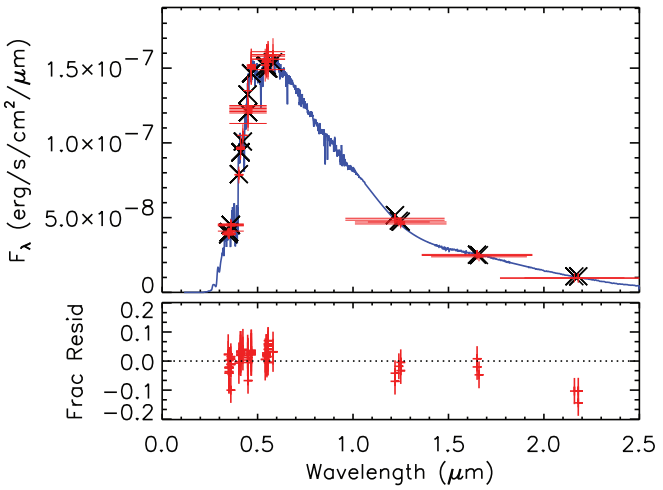

Figure 2. SED fit for 55 Cnc. The (blue) spectrum is a G9IV spectral template (Pickles 1998). The (red) crosses indicate photometry values from the literature. "Error bars" in x-direction represent bandwidths of the filters used. The (black) X-shaped symbols show the flux value of the spectral template integrated over the filter transmission. The lower panel shows the residuals around the fit in fractional flux units of photometric uncertainty. For details, see Section 3.

(A color version of this figure is available in the online journal.)

Our values for 55 Cnc's stellar mass and age are consistent with their respective counterparts obtained via spectroscopic analysis combined with photometric bolometric corrections (Valenti & Fischer 2005), as well as with age estimates using the Ca II chromospheric activity indicators and gyrochronology relations (Wright et al. 2004; Mamajek & Hillenbrand 2008). In addition, they are within the error bars of the equivalent values derived in Fischer et al. (2008) and the ones used in Winn et al. (2011) and Demory et al. (2011). Finally, the stellar surface gravity is computed from our radius measurement and mass estimate, plus associated uncertainties, to be $\log g = 4.45 \pm 0.01$.

A summary of all directly determined and calculated stellar astrophysical parameters in this section is reported in Table 1.

4. 55 CANCRI'S HABITABLE ZONE

In this section, we calculate the location and extent of the HZ in the 55 Cnc system, and we examine which of the orbiting planets spend all or part of their respective orbits in the HZ. We further comment on the potential existence of habitable objects around 55 Cnc.

A circumstellar traditional HZ is defined as the range of distances from a star at which a planet with a moderately dense atmosphere could harbor liquid water on its surface. More details about the definition of HZs, typically used for Earth-like planets with clearly defined surfaces, can be found in Kasting et al. (1993) and Underwood et al. (2003).

Our calculations of the inner and outer boundaries of 55 Cnc's HZ are based on our directly determined host star properties (Section 3). Similar to von Braun et al. (2011a) for GJ 581, we use the equations in Underwood et al. (2003) and Jones & Sleep (2010) to relate inner and outer edges of the HZ to the luminosity and effective temperature of the host star 55 Cnc. We find an inner and outer HZ boundary of 0.67 AU and 1.32 AU, respectively. The HZ is shown as the gray shaded region in

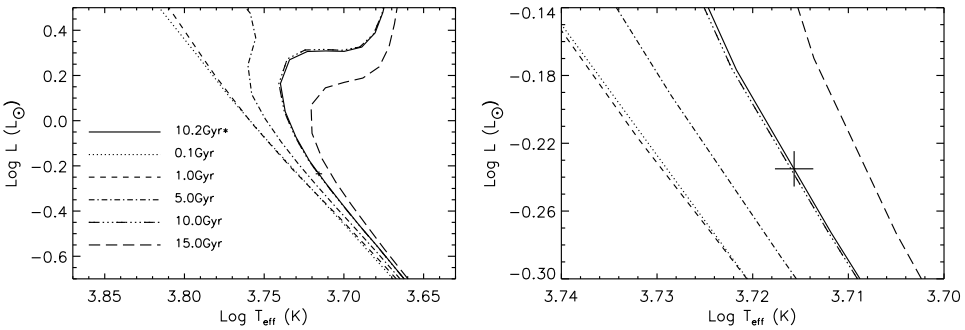

Figure 3. Comparison of our values of 55 Cnc's L and $T_{\rm EFF}$ to Yonsei–Yale isochrones. The right panel is a zoom of the left panel, centered on the data point. Different age isochrones are indicated by the different line styles, where the best-fit isochrone (asterisk; solid line) yields a stellar age of 10.2 ± 2.5 Gyr. For details, see Section 3.3 and Table 1.

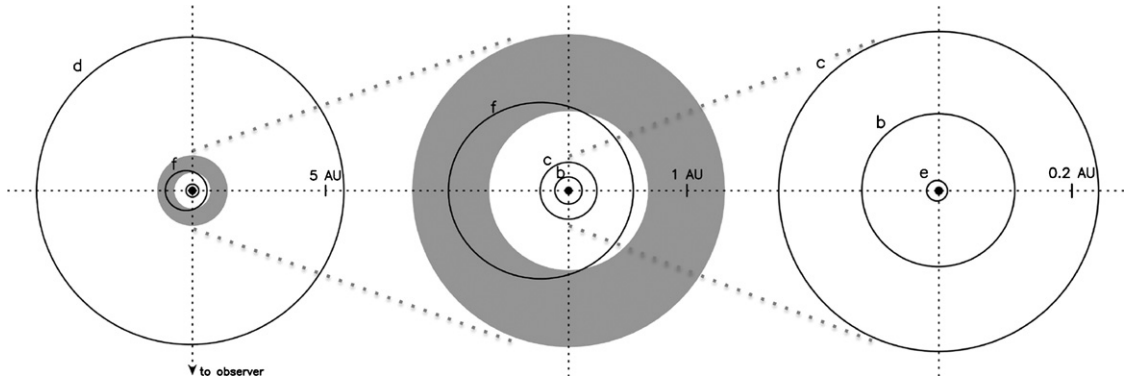

Figure 4. Top-down view of the 55 Cnc system, showing the full orbital architecture centered on the star at increasing zoom levels from left to right (note different scales on ordinate). The habitable zone is indicated by the gray shaded region. Orbital element values are adopted from Table 10 in Dawson & Fabrycky (2010). Planet d is well beyond the outer edge of the HZ (left panel). Planet f periodically dips into and out of the HZ during its elliptical ($e \simeq 0.3$) orbit (left and middle panels). See also von Braun et al. (2011b). Planets b, c, and e (the transiting super-Earth) are well inside the system's HZ (right panel). For details, see Section 4 and Table 2.

Figure 4, which illustrates the architecture of the 55 Cnc system at different spatial scales.

We calculate equilibrium temperatures $T_{\rm eq}$ for the five known 55 Cnc planets using the equation

$$T_{\rm eq}^4 = \frac{S(1-A)}{f\sigma}, \quad (2)$$

where S is the stellar energy flux received by the planet, A is the Bond albedo, and σ is the Stefan–Boltzmann constant (Selsis et al. 2007). The energy redistribution factor f indicates the atmospheric efficiency of redistributing the radiation received from the parent star across the planetary surface by means of circulation, winds, jet streams, etc. f is set to 2 for a hot day side (no heat redistribution between day and night side) and to 4 for even heat distribution.[14] Table 2 shows the calculated equilibrium temperatures for the planets in the 55 Cnc system assuming different values of Bond albedos, including the value for Earth ($A = 0.29$). Note that the temperature given for the $f = 2$ scenario is the planet dayside temperature. All of 55 Cnc's known planets, except planet f, are either located well inside or beyond the system's HZ (see Figure 4).

Figure 4 shows that planet 55 Cnc f ($M \sin i = 0.155\, M_{\rm Jupiter} = 49.3\, M_{\oplus}$; Table 10 in Dawson & Fabrycky 2010) is on an elliptical orbit ($e \simeq 0.3$) during which it spends about 74% of its orbital period of approximately 260 days inside the HZ. Thus, $T_{\rm eq}$ is a function of time (or phase angle). The time-averaged distance between planet f and 55 Cnc is 0.82 AU. For the $f = 2$ scenario (no heat redistribution between day and night sides) and $A = 0.29$, planet f's time-averaged dayside temperature is 294 K, and varies between 263 K (apastron) and 359 K (periastron) during its elliptical orbit. Assuming an even heat redistribution ($f = 4$) and $A = 0.29$, however, we calculate planet f's time-averaged surface temperature $T_{\rm eq}^{f=4} = 247$ K, with a variation of 221 K at apastron to 302 K at periastron. Planet f's long-period, elliptical orbit makes any kind of tidal synchronization unlikely. Further taking into account its mass, typical of gas giant planets, $f = 4$ appears to be a much more likely scenario than $f = 2$ or similar. Note, that even though planet f's time-averaged $T_{\rm eq}^{f=4}$ is below the freezing point of water, heating due to greenhouse gases could moderate temperatures in its atmosphere to above the freezing point of water (e.g., Selsis et al. 2007; Wordsworth et al. 2010).

We point out that eccentricity estimates for planet f range from values between 0.13 and 0.3 in Dawson & Fabrycky (2010) for the correct 0.74 day period of planet e with 1σ error bars of $\sim$0.05 (in e_f). Clearly, the differences between the temperatures at apastron and periastron calculated above decrease if e_f is smaller than our value of 0.3. In addition, the orbit-averaged flux S (Equation (2)) increases with the planetary eccentricity e as $(1-e^2)^{-1/2}$. Thus, the equilibrium temperature of planet f increases for larger e_f, but this is at most a 10% effect for $e_f < 0.4$. Finally, irrespective of the instantaneous value of e_f, all the planets in the 55 Cnc system undergo long-term secular oscillations in eccentricity such that their effective temperatures may change in time.

We further note that the planet 55 Cnc f is likely too massive to harbor liquid water on any planetary surface (Selsis et al. 2007). In terms of an actual *habitable object* in the 55 Cnc system, there are thus two potential candidates: a massive moon in

[14] See the Appendix in Spiegel & Burrows (2010) for a detailed explanation of the f parameter.

Table 2
Equilibrium Temperatures for the 55 Cnc System Planets

Planet			$A = 0.1$		$A = 0.29$		$A = 0.5$	
	$M_{\sin i}$ ($M_{\rm Jup}$)	a (AU)	$T_{\rm eq}^{f=4}$ (K)	$T_{\rm eq}^{f=2}$ (K)	$T_{\rm eq}^{f=4}$ (K)	$T_{\rm eq}^{f=2}$ (K)	$T_{\rm eq}^{f=4}$ (K)	$T_{\rm eq}^{f=2}$ (K)
b	0.825(3)	0.1148(8)	699 ± 4	831 ± 5	659 ± 4	784 ± 5	604 ± 4	718 ± 5
c	0.171(4)	0.2403(17)	483 ± 3	575 ± 4	456 ± 3	542 ± 4	417 ± 3	496 ± 4
d	3.82(4)	5.76(6)	99 ± 1	117 ± 1	93 ± 1	111 ± 1	85 ± 1	101 ± 1
e	0.0260(10)	0.01560(11)	1895 ± 12	2253 ± 14	1786 ± 12	2124 ± 14	1636 ± 12	1945 ± 14
f	0.155(8)	0.781(6)	268 ± 2	319 ± 2	253 ± 2	301 ± 2	231 ± 2	275 ± 2

Notes. Equilibrium temperatures for different values of the Bond albedo A, and based on the equations in Selsis et al. (2007). $A = 0.29$ corresponds to Earth's albedo. Planet masses and orbital element values are from Table 10 in Dawson & Fabrycky (2010); note that 55 Cnc e's mass is not subject to a sin i uncertainty. $f = 4$ implies perfect energy redistribution efficiency on the planetary surface, $f = 2$ means no energy redistribution between day and night sides. For details, see Section 4 and Figure 4. The uncertainties in $T_{\rm eq}$ are based on the uncertainties in 55 Cnc's luminosity and the planets' orbital elements. Planet f's elliptical orbit ($e \simeq 0.3$) causes it to spend around 74% of its year in 55 Cnc's circumstellar HZ (Figure 4). For details, see Section 4.

orbit around planet f or an additional low-mass planet in or near the HZ.

Could 55 Cnc f host a potentially habitable moon? One formation model suggests that the mass of a giant planet satellite should generally be about 10^{-4} times the planet mass (Canup & Ward 2006). For 55 Cnc f the expected satellite mass is therefore $\sim 5 \times 10^{-3}\ M_{\oplus}$, which is comparable to the mass of Jupiter's moon Europa but probably too low to retain a thick atmosphere for long timescales at HZ temperatures (Williams et al. 1997). Of course, there exist alternate origin scenarios that could produce more massive giant planet moons (e.g., Agnor & Hamilton 2006) with correspondingly higher probability of atmospheric retention. In addition, values of $e_f < 0.3$ would slightly decrease the equilibrium temperature of any hypothetical moon around planet f, and consequently increase its potential of retaining an atmosphere.

Any potential, dynamically stable existence of an additional low-mass planet in the outer part of 55 Cnc's HZ depends in large part on the eccentricity of planet f, since its gravitational reach will cover a larger fraction of the HZ for higher values of e_f. Using the simple scaling arguments of Jones et al. (2005), which are based on the analytical two-planet Hill stability limit (Marchal & Bozis 1982; Gladman 1993), the semimajor axis of the orbit closest to planet f that is likely to be stable for a low-mass planet is roughly 0.87/1.0/1.14/1.24/1.32 AU for e_f = 0/0.1/0.2/0.3/0.4. Given our calculated value of 1.32 AU for the outer edge of the HZ and our default value of $e_f = 0.3$, only the outermost portion of the HZ is able to host an additional low-mass planet.

This simple scaling argument matches up reasonably well with the N-body simulations of Raymond et al. (2008), who mapped the stable zone of 55 Cnc between planets f and d but assumed a low fixed (initial) value for e_f. The exterior 3:2 mean motion with planet f, located at 1.02–1.04 AU, represents an additional stable niche. Raymond et al. (2008) showed that, although narrow, this resonance is remarkably stable for long timescales, for planet masses up to the mass of planet f or even larger, and even for some orbits that are so eccentric that they cross the orbit of planet f. This resonance is stable whether planet f's orbit is eccentric or circular.

Thus, we conclude that if e_f is large ($\gtrsim$0.3) an additional Earth-like planet could exist in either the 3:2 resonance with planet f at 1.03 AU or in the outer reaches of the HZ. In that case the additional planet's orbit would likely also be eccentric, although climate models have shown that large eccentricities do not preclude habitable conditions (Williams & Pollard 2002; Dressing et al. 2010). If, however, e_f is small then an additional planet in HZ could be as close in as about 0.9 AU and would likely be on a low-eccentricity orbit.

5. THE TRANSITING SUPER-EARTH 55 Cnc e

This section contains the implications of our calculated stellar parameters for the radius and bulk density of the transiting super-Earth 55 Cnc e.

Three recent papers rely on the value of 55 Cnc's physical stellar radius that we measure to be $0.943 \pm 0.010\ R_{\odot}$ (see Section 3.1 and Table 1). Winn et al. (2011) and Demory et al. (2011) both independently report the photometric detection of a transit of 55 Cnc e. In addition, Kane et al. (2011) calculate combinations of expected planetary brightness variations with phase, for which knowledge of planetary radius is useful.

In our calculations of the planetary radius, we assume that 55 Cnc e has a cold night side, i.e., the planet is an opaque spot superimposed onto the stellar disk during transit. We note that, strictly speaking, any calculated planetary radius therefore actually represents a lower limit, but due to the intense radiation received by the parent star at this close proximity, it is unlikely for 55 Cnc e to retain any kind of atmosphere (Winn et al. 2011). Using the formalism in Winn (2010), the measured flux decrement during transit therefore corresponds to $(R_p/R_{\star})^2$, where R_p and $R_{\star}$ are planetary and stellar radius, respectively.

Winn et al. (2011) obtain $R_p/R_{\star} = 0.0195 \pm 0.0013$ and $M_p = 8.63 \pm 0.35\ M_{\oplus}$. In combination with our stellar radius, these measurements result in $R_p = 2.007 \pm 0.136\ R_{\oplus}$ and a planetary bulk density of 5.882 ± 0.728 g cm^{-3} or $1.067 \pm 0.132\ \rho_{\oplus}$.

Demory et al. (2011) measure $R_p/R_{\star} = 0.0213 \pm 0.0014$ and assume a planetary mass of $7.98 \pm 0.69\ M_{\oplus}$. Together with our radius for 55 Cnc, they imply a planetary radius of $2.193 \pm 0.146\ R_{\oplus}$ and a bulk density of 4.173 ± 0.602 g cm^{-3}, corresponding to $0.757 \pm 0.109\ \rho_{\oplus}$.[15]

We refer the reader to the planet transit discovery papers, in particular Figure 3 in Winn et al. (2011) and Figures 5 and 6 in Demory et al. (2011), for comparison of these density values to other transiting super-Earths in the literature. It should be noted that, although 55 Cnc is the brightest known star with a transiting planet, the amplitude of the transit signal is among the smallest known to date, making the determination of planet radius very difficult.

[15] We note that we are calculating uncertainties based on simple Gaussian error propagation. That is, we make the assumption that the errors are not correlated, which is not quite correct since, e.g., stellar mass can be related to stellar radius.

6. SUMMARY AND CONCLUSION

Characterization of exoplanets is taking an increasingly central role in the overall realm of planetary research. An often overlooked aspect when determining the characteristics of extrasolar planets is that reported physical quantities are actually dependent on the astrophysical parameters of the respective host star, and that assumptions of varying degrees of certainty may implicitly be contained in quoted absolute values of exoplanet parameters. Consequently, the necessity of "understanding the parent stars" can hardly be overstated, and it served as the principal motivation for the research presented here.

Our new interferometric measurements provide a directly determined, high-precision angular radius for the host star 55 Cnc. We couple these measurements with trigonometric parallax values and literature photometry to obtain the stellar physical diameter ($0.943 \pm 0.010\,R_{\odot}$), effective temperature (5196 ± 24 K), luminosity ($0.582 \pm 0.014\,L_{\odot}$), and characteristics of the HZ (see Table 1). This shows that planet f spends 74% of its year in the HZ. We use isochrone fitting to calculate 55 Cnc's age (10.2 ± 2.5 Gyr) and mass ($0.905 \pm 0.015\,M_{\odot}$). Finally, the directly determined stellar radius allows for a model-independent estimate of the radius of any transiting extrasolar planets. We use our stellar diameter value and recently published numbers for $R_p/R_{\star}$ to estimate the radius ($\sim 2.05 \pm 0.15\,R_{\oplus}$) and bulk density (0.76 or 1.07 $\rho_{\oplus}$, depending on the assumed planetary mass) of the transiting planet 55 Cnc e.

Due to its (naked-eye) brightness and consequent potential for detailed spectroscopic studies, the small size of the transiting super-Earth 55 Cnc e, planet f's location in the circumstellar HZ, and generally the fact that 55 Cnc hosts at least five planets at a wide range of orbital distances, the system will undoubtedly be the source of exciting exoplanet results in the very near future.

The authors thank B.-O. Demory and J. N. Winn for many open conversations and exchange of extremely useful information about the planetary radius of 55 Cnc e during the preparation of this manuscript, E. K. Baines for discussions about interferometric data quality, and D. Spiegel for very helpful suggestions on the issues interferometric visibilities and planet habitability. We would further like to extend our gratitude to the anonymous referee for careful reading of the manuscript and the insightful comments that improved the quality of this publication. T.S.B. acknowledges support provided by NASA through Hubble Fellowship grant #HST-HF-51252.01 awarded by the Space Telescope Science Institute, which is operated by the Association of Universities for Research in Astronomy, Inc., for NASA, under contract NAS 5-26555. S.T.R. acknowledges partial support from NASA grant NNH09AK731. The CHARA Array is funded by the National Science Foundation through NSF grants AST-0606958 and AST-0908253 and by Georgia State University through the College of Arts and Sciences, the W. M. Keck Foundation, the Packard Foundation, and the NASA Exoplanet Science Institute. This research made use of the SIMBAD literature database, operated at CDS, Strasbourg, France, and of NASA's Astrophysics Data System. This publication makes use of data products from the Two Micron All Sky Survey, which is a joint project of the University of Massachusetts and the Infrared Processing and Analysis Center/California Institute of Technology, funded by the National Aeronautics and Space Administration and the National Science Foundation. This research made use of the NASA/IPAC/NExScI Star and Exoplanet Database, which is operated by the Jet Propulsion Laboratory, California Institute of Technology, under contract with the National Aeronautics and Space Administration.

REFERENCES

Agnor, C. B., & Hamilton, D. P. 2006, Nature, 441, 192
Argue, A. N. 1963, MNRAS, 125, 557
Argue, A. N. 1966, MNRAS, 133, 475
Arribas, S., & Martinez Roger, C. 1989, A&A, 215, 305
Baines, E. K., McAlister, H. A., ten Brummelaar, T. A., et al. 2008, ApJ, 680, 728
Boden, A. F., van Belle, G. T., Colavita, M. M., et al. 1998, ApJ, 504, L39
Butler, R. P., Marcy, G. W., Williams, E., Hauser, H., & Shirts, P. 1997, ApJ, 474, L115
Canup, R. M., & Ward, W. R. 2006, Nature, 441, 834
Claret, A. 2000, A&A, 363, 1081
Cowley, A. P., Hiltner, W. A., & Witt, A. N. 1967, AJ, 72, 1334
Cutri, R. M., Skrutskie, M. F., van Dyk, S., et al. 2003, The 2MASS All Sky Catalog of Point Sources (Pasadena: IPAC)
Dawson, R. I., & Fabrycky, D. C. 2010, ApJ, 722, 937
Demarque, P., Woo, J.-H., Kim, Y.-C., & Yi, S. K. 2004, ApJS, 155, 667
Demory, B., Gillon, M., Deming, D., Valencia, D., et al. 2011, arXiv:1105.0415
Dressing, C. D., Spiegel, D. S., Scharf, C. A., Menou, K., & Raymond, S. N. 2010, ApJ, 721, 1295
Eggen, O. J. 1978, ApJS, 37, 251
Fischer, D. A., Marcy, G. W., Butler, R. P., et al. 2008, ApJ, 675, 790
Gezari, D. Y., Pitts, P. S., & Schmitz, M. 1999, VizieR Online Data Catalog, 2225, 0
Gladman, B. 1993, Icarus, 106, 247
Gonzalez, G., & Piche, F. 1992, AJ, 103, 2048
Gray, R. O., Corbally, C. J., Garrison, R. F., McFadden, M. T., & Robinson, P. E. 2003, AJ, 126, 2048
Hanbury Brown, R., Davis, J., Lake, R. J. W., & Thompson, R. J. 1974, MNRAS, 167, 475
Hauck, B., & Mermilliod, M. 1998, A&AS, 129, 431
Jones, B. W., & Sleep, P. N. 2010, MNRAS, 407, 1259
Jones, B. W., Underwood, D. R., & Sleep, P. N. 2005, ApJ, 622, 1091
Kane, S. R., Ciardi, D. R., Dragomir, D., Gelino, D. M., & von Braun, K. 2011, arXiv:1105.1716
Kasting, J. F., Whitmire, D. P., & Reynolds, R. T. 1993, Icarus, 101, 108
Kazlauskas, A., Boyle, R. P., Philip, A. G. D., et al. 2005, Balt. Astron., 14, 465
Kim, Y.-C., Demarque, P., Yi, S. K., & Alexander, D. R. 2002, ApJS, 143, 499
Mamajek, E. E., & Hillenbrand, L. A. 2008, ApJ, 687, 1264
Marchal, C., & Bozis, G. 1982, Celest. Mech., 26, 311
Marcy, G. W., Butler, R. P., Fischer, D. A., et al. 2002, ApJ, 581, 1375
Marlborough, J. M. 1964, AJ, 69, 215
McArthur, B. E., Endl, M., Cochran, W. D., et al. 2004, ApJ, 614, L81
Mermilliod, J.-C. 1986, Catalogue of Eggen's UBV Data, 0, 0
Niconov, V. B., Nekrasova, S. V., Polosuina, N. S., Rachkouvsky, N. D., & Chuvajev, W. K. 1957, Izv. Ordena Tr. Krasnogo Znameni Krymskoj Astrofiz. Obs., 17, 42
Olsen, E. H. 1983, A&AS, 54, 55
Olsen, E. H. 1993, A&AS, 102, 89
Persson, S. E., Aaronson, M., & Frogel, J. A. 1977, AJ, 82, 729
Pickles, A. J. 1998, PASP, 110, 863
Raymond, S. N., Barnes, R., & Gorelick, N. 2008, ApJ, 689, 478
Rufener, F. 1976, A&AS, 26, 275
Selsis, F., Kasting, J. F., Levrard, B., et al. 2007, A&A, 476, 1373
Spiegel, D. S., & Burrows, A. 2010, ApJ, 722, 871
ten Brummelaar, T. A., McAlister, H. A., Ridgway, S. T., et al. 2005, ApJ, 628, 453
Underwood, D. R., Jones, B. W., & Sleep, P. N. 2003, Int. J. Astrobiol., 2, 289
Valenti, J. A., & Fischer, D. A. 2005, ApJS, 159, 141
van Belle, G. T., Ciardi, D. R., & Boden, A. F. 2007, ApJ, 657, 1058
van Belle, G. T., & von Braun, K. 2009, ApJ, 694, 1085
van Leeuwen, F. (ed.) 2007, in *Hipparcos*, the New Reduction of the Raw Data (Astrophysics and Space Science Library, Vol. 350; Dordrecht: Springer), 20
von Braun, K., Boyajian, T. S., Kane, S. R., et al. 2011a, ApJ, 729, L26
von Braun, K., Boyajian, T. S., ten Brummelaar, T. A., et al. 2011b, arXiv:1107.1936
Williams, D. M., Kasting, J. F., & Wade, R. A. 1997, Nature, 385, 234
Williams, D. M., & Pollard, D. 2002, Int. J. Astrobiol., 1, 61
Winn, J. N. 2010, arXiv:1001.2010
Winn, J. N., Matthews, J. M., Dawson, R. I., et al. 2011, ApJ, 737, L18
Wordsworth, R. D., Forget, F., Selsis, F., et al. 2010, A&A, 522, A22
Wright, J. T., Marcy, G. W., Butler, R. P., & Vogt, S. S. 2004, ApJS, 152, 261
Yi, S., Demarque, P., Kim, Y.-C., et al. 2001, ApJS, 136, 417